Dalton Transactions

ROYAL SOCIETY OF CHEMISTRY

PAPER

View Article Online
View Journal | View Issue



Cite this: *Dalton Trans.*, 2023, **52**, 12461

# Investigation on the predictive power of tolerance factor $\tau$ for A-site double perovskite oxides†

Elisabeth K. Albrecht and Antti J. Karttunen *

Received 26th June 2023,
Accepted 14th August 2023

DOI: 10.1039/d3dt01990j

rsc.li/dalton

We have used a recently introduced new tolerance factor $\tau$ to create a stability map of all possible A-site double perovskite titanates $AA'Ti_2O_6$ and niobates $AA'Nb_2O_6$. The predictive power of $\tau$ is relatively good based on comparisons with available experimental data for A-site double perovskites. We carried out quantum chemical calculations on two hypothetical double perovskite compositions $CsScTi_2O_6$ and $YRbTi_2O_6$, where $\tau$ predicts high probability for their existence. In both cases, we found limits in the predictive power of the new tolerance factor for ion combinations on the A and A′ site which are very different in size. A difference in oxidation state may decrease the accuracy, as well. Overall, the A-site double perovskite stability mapping provides a starting point for the discovery of novel A-site double perovskites.



## 1. Introduction

Crystal structure prediction for compounds such as perovskites is still a challenging task due to the variety of compositions and structural modifications they can adapt. The general structural formula $ABX_3$ with the space group $Pm\bar{3}m$ for ideal perovskites has the A cation on the corners of a primitive cubic unit cell, while the B cation sits in the center. The X anion occupies the face centers, leading to an octahedral coordination of the B cation. The $BX_6$ octahedra are corner-sharing and can tilt and distort due to for example size mismatch in the cations.[1] The size mismatches and resulting structural effects make it difficult to predict the existence and crystal structure of perovskites. Goldschmidt suggested a tolerance factor $t$

$$t = \frac{r_A + r_X}{\sqrt{2}(r_B + r_X)} \quad (1)$$

which includes the ionic radii $r_A$, $r_B$ and $r_X$ of the A, B and X ion, respectively, to determine if certain ions will form a perovskite or not.[2] The Goldschmidt tolerance factor $t$ is derived from simple geometrical considerations which do not take the rotation or distortion of the $BX_6$ octahedra into account. In order to achieve a more comprehensive picture of the formability of perovskites, an octahedral factor $\mu$

$$\mu = \frac{r_B}{r_X} \quad (2)$$

has been derived, accounting for tilting of the octahedra.[3] At the same time, the need to consider two parameters $\mu$ and $t$ already makes it more complicated to make rigorous predictions. While the tolerance factor $t$ is very easy to apply because it is based on ionic radii only, its accuracy can be poor. The ideal $ABX_3$ perovskite structure has $t = 1$, where the space is optimally filled. This is rarely the case and perovskites in cubic, tetragonal, or orthorhombic crystal systems can be expected for $0.825 \leq t \leq 1.059$[4] due tilting and distortion of octahedra as well as displacement of cations. For $t > 1.059$, a hexagonal perovskite-like structure is expected, and for $t < 0.825$ other structure types such as ilmenite are more likely. Overall, the tolerance factor $t$ correctly predicts only about 74%[4] of the materials as perovskites or non-perovskites. Therefore, Bartel *et al.*[4] have suggested a new tolerance factor $\tau$

$$\tau = \frac{r_X}{r_B} - n_A\left(n_A - \frac{r_A/r_B}{\ln(r_A/r_B)}\right) \quad (3)$$

where $r_A$, $r_B$, and $r_X$ are ionic radii (by definition $r_A > r_B$), and the oxidation state of the A-ion is $n_A$. The tolerance factor $\tau$ was identified by the Sure Independence Screening and Sparsifying Operator (SISSO) method.[5] A machine learning framework trained by known perovskite crystal structures identified the most descriptive parameters of the crystal structures. Similar to $t$, the formula for $\tau$ contains the ionic radii, but in addition

*Department of Chemistry and Materials Science, Aalto University, P.O. Box 16100, FI-00076 Aalto, Finland. E-mail: antti.karttunen@aalto.fi*

†Electronic supplementary information (ESI) available: Database of investigated double perovskite oxide compositions in Excel format, optimized structures in CIF format, and absolute electronic energies of the studied systems. See DOI: https://doi.org/10.1039/d3dt01990j

it includes information on the oxidation state of the A-ion. Both $t$ and $\tau$ are derived for simple $ABX_3$ perovskites. To make predictions on double perovskites, the average ionic radius of both ions on the A- or B site is used together with the average oxidation state of the A ions, if applicable. This makes the predictive power of the tolerance factor $t$ even smaller, while the performance of $\tau$ is still rather high as shown by Bartel *et al.* for B-site ordered double perovskites.[4] Looking at simple perovskites, the tolerance factor $\tau$ distinguished correctly between perovskite and non-perovskite for 92% of the materials in the experimental set of 576 compounds. For B-site ordered double perovskites, a 91% accuracy was reported for a set of 918 $A_2BB'X_6$ compounds. As an overall outcome, Bartel *et al.* used $\tau$ to determine the probability $P(\tau)$ of a compound being a perovskite by Platt's scaling.[6]

In 2018, Filip and Giustino[7] screened ions in 2291 known compounds for their ability to form B-site ordered double perovskites using the average B-ion radius together with tolerance factor $t$. The screening was based on Goldschmidt's non-rattling principle which is also the basis of the Goldschmidt tolerance factor $t$. The octahedral factor $\mu$ was divided into the average octahedral factor $\bar{\mu} = (r_B + r'_B)/(2r_X)$ and the octahedral mismatch factor $\Delta\mu = |r_B - r'_B|/(2r_X)$. These three parameters were then used to predict 94 232 hitherto-unknown perovskites.

While B-site ordered double perovskites have been investigated in several tolerance factor-based high-throughput screening studies, A-site ordered double perovskites (Fig. 1) have received less attention. No high-throughput screening studies on the existence or crystal structure of A-site (ordered) double perovskites have been carried out, in particular with respect to the potential ordering of the A-site cations. It is relatively difficult to predict whether two different ions on the A-site will order or not. In fact, considering the relatively small number of A-site ordered double perovskites it is more likely that the A-site ions will not order. However, as an initial screening approach, compositions with two different ions on the A-site can in any case be considered. A screening of potential A-site double perovskites gives an idea about how well the new tolerance factor $\tau$ works for A-site double perovskites when comparing the predictions with known compounds. Furthermore, such screening can be used to predict potential compositions that might be worth investigating experimentally.

Various functional properties such as ferroelectricity, pyroelectricity, superconductivity, and ferromagnetism make perovskites an important materials research platform due to high demand on materials with very specific functionalities.[9–11] By extending the perovskite compositions from simple to double perovskites, their properties can be further fine-tuned by combining different ions. While there has been a significant research focus on B-site ordered double perovskites,[12] A-site ordered double perovskites have been studied less.[13–26] Here, we aim to provide a starting point to make predictions on the crystal structures of new A-site ordered double perovskites ($AA'B_2O_6$). For this purpose, we have compiled a database of possible A-site double perovskite compositions and applied the new tolerance factor $\tau$ of Bartel *et al.* to measure the probability of obtaining a double perovskite for each composition. We have also carried out quantum chemical calculations on several promising compositions based on $\tau$ to investigate the strengths and weaknesses of this tolerance factor when applied to A-site double perovskites.

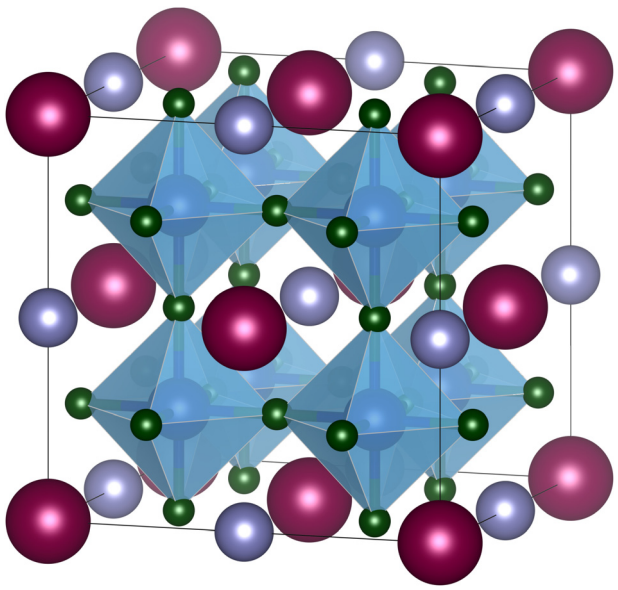

Fig. 1 A-site ordered double perovskite $AA'B_2X_6$ with rock-salt ordering of the A-site cations. A cations colored in dark red, A′ cations in purple, B cations in blue, and X anions in green. Figure created with VESTA.[8]

## 2. Methods

### 2.1. Data acquisition

First, we built a database of possible compositions for A-site ordered double perovskites. For the A-site, we included all metals with an atomic number ≤83, except for technetium. For the B-site, we chose niobium (+V) and titanium (+IV), as they are common B-site ions in perovskites. They can also show second-order Jahn–Teller effect which supports layered ordering in A-site ordered double perovskites.[13] From this set of elements, we removed all combinations for the A-site which did not lead to a zero net charge with the chosen B-ions. Similar to Bartel *et al.*[4] in the case of $A_2BB'O_6$ double perovskites, we used the Shannon ionic radii for the calculation of $\tau$.[27] Since the ionic radii depend on the coordination number of the ion, we chose to use the 12-coordinated ionic radius for the A-site cations if available. In those cases where there was no 12-coordination available, we chose the ionic radius of the coordination closest to twelve, in line with Bartel *et al.* In reality, the ion may not form a structure with such high coordination number and this would be accounted for by a tilt of the oxygen octahedra, which may also change the coordination of the oxygen anions from six to a smaller number. However, the

ionic radius of oxygen was kept the same for all evaluated compositions (1.4 Å, corresponding to coordination number six).

In addition to the ionic radius choices discussed above, we also evaluated another approach: if a 12-coordinated ionic radius was not available for an ion, we estimated it from Bond Valence Sum (BVS) calculations using

$$V_i = \exp\left(\frac{R_{ij} - d_{ij}}{b}\right) \quad (4)$$

where the BVS $V_i$ is set to be 1/12, 1/6 and 1/4 for twelve equal bonds and oxidation states of +I, +II, and +III, respectively.[28] The constant $b$ is, as it is common, set to 0.37 Å. The bond valence parameters $R_{ij}$ are taken from Brown and Lufaso.[29] For Au(+I), Ta(+III), Ti(+II), and Tm(+II) we were unable to find bond valence parameters. Inorganic Crystal Structure Database (ICSD) was used as a reference on whether a certain composition already exists as a perovskite or a non-perovskite.[30] All data and calculations to obtain the $\tau$ values discussed here are included as ESI.†

To get the probability of forming a perovskite with a certain composition, we fitted the calculated values of $\tau$ to the Platt-scaled classification probabilities of Bartel *et al.*[4] Next, we translated the probabilities to a color scale and constructed a map out of them. In those cases where multiple ionic combinations with the same elements were possible, we used the average probability. For example in the case of $AuTlTi_2O_6$, both Au and Tl can have the oxidation state of +I or +III which leads to different average ionic radii and thus to different values of $\tau$. The probabilities obtained for such combinations do not differ much, which is why we chose to use the average value. In the case of $AuTlTi_2O_6$, the probabilities are 58% for Au(III)/Tl(I) and 52% for Au(I) and Tl(III). This averaging applies to five combinations, $CoCuTi_2O_6$, $CuEuTi_2O_6$, $MnCuTi_2O_6$, $TiCuTi_2O_6$, and $AuTlTi_2O_6$.

### 2.2. Computational details

For the quantum chemical calculations, CRYSTAL17[31] program package was used. We applied hybrid PBE0 density functional method, (DFT-PBE0)[32,33] in combination with all-electron, Gaussian-type basis sets based on Karlsruhe def2 sets.[34] Triple-ζ-valence + polarization (TZVP) quality basis sets for O, Sc, Ti, Y, and Nb were taken from ref. 35. Split-valence + polarization(SVP) quality basis sets for K, Rb, and Cs were taken from ref. 36. The Monkhorst–Pack type $k$-meshes used to sample the reciprocal space are similar to our previous paper on $CaMnTi_2O_6$ double perovskite.[37,38] In all calculations, default DFT integration grids and optimization convergence thresholds of CRYSTAL17 were applied. The calculations were carried out with Coulomb and exchange integral tolerance factors (TOLINTEG) set to tight values of 8, 8, 8, 8, and 16. All reported relative energies are based on electronic energies obtained at 0 K, Gibbs Free Energies have not been considered. Harmonic frequency calculations were carried out on selected crystal structures with the approach implemented in CRYSTAL.[39,40]

## 3. Results and discussion

### 3.1. Overview of the possible A-site double perovskites based on $\tau$

The map in Fig. 2 provides an overview of possible A-site double perovskites and their probability of forming a perovskite titanate (upper triangle) or niobate (lower triangle). The probabilities are based on tolerance factor $\tau$ (eqn (3)). Since A-site double perovskites are less studied than B-site ordered double perovskites, the map gives a starting point for choosing potential new AA′ combinations in an $AA'B_2O_6$ double perovskite. The darker the field in Fig. 2, the higher the probability of forming a perovskite based on the tolerance factor $\tau$. Due to the oxidation state of +V of niobium, there are only few possible combinations for A-site ions in the lower triangle. When the B-site is occupied by Nb, both the A and A′ ion must have an oxidation state of +I. When the B-site is occupied by Ti in oxidation state +IV, there is a larger variety of ionic combinations. Combinations of oxidation states II/II, I/III, and III/I are possible. We note that the map does not provide information of whether the A-site ions will order in a certain way or if they will be disordered, forming a solid solution.

Based on the tolerance factor $\tau$, the most likely A-site double perovskites are expected for cases where the A- and A′-site are filled with an alkali metal in combination with a d-metal or a lanthanide. The larger the alkali metal cation, the more likely the perovskite, which makes compositions with Cs the most likely ones. According to Bartel *et al.*,[4] a perovskite is expected if $\tau < 4.18$. The most likely composition, with the smallest positive $\tau$ value of 3.751 is $CsLaTi_2O_6$, which has not been experimentally observed yet. In the case of $CsLaTi_2O_6$, the difference in oxidation state of cesium(I) and lanthanum (III), as well as the difference in ionic radii of about 0.52 Å suggests an A-site ordered perovskite.[14] Since gold can show oxidation states I, II, and III, it forms many possible combinations. Here, again, those with the lanthanides and alkali metals are the most likely ones as in $AuLaTi_2O_6$ and $CsAuTi_2O_6$ with $\tau = 3.860$.

The map in Fig. 2 has been drawn based on Shannon ionic radii only, but the use of BVS-derived radii for the ions that do not have a 12-coordinated Shannon radii changes most of the $\tau$ values close to 4.18 only by few percent, leading only in small changes in probability. A more significant change can be seen for six negative $\tau$ values, where the average ionic radius of A and A′ is smaller than the ionic radius of the B ion (Table S1 in ESI†). These are $LiBTi_2O_6$, $BeZnTi_2O_6$, $BeCuTi_2O_6$, $BeGeTi_2O_6$, $BeNiTi_2O_6$, and $CuBTi_2O_6$. The map in Fig. 2 does not take these compositions into account since they do not fulfil the definition of $r_A > r_B$. Geometrically, this definition makes sense and we do not expect those combinations to be likely. When using BVS-derived radii for Li, Be, and B, the $\tau$ values become large and positive, suggesting the compositions to be highly unlikely.

As mentioned above, a perovskite is expected if $\tau < 4.18$. Out of the 208 predicted A-site double perovskites with $\tau <$ 4.18, 26 have been synthesized and characterized as perovs-

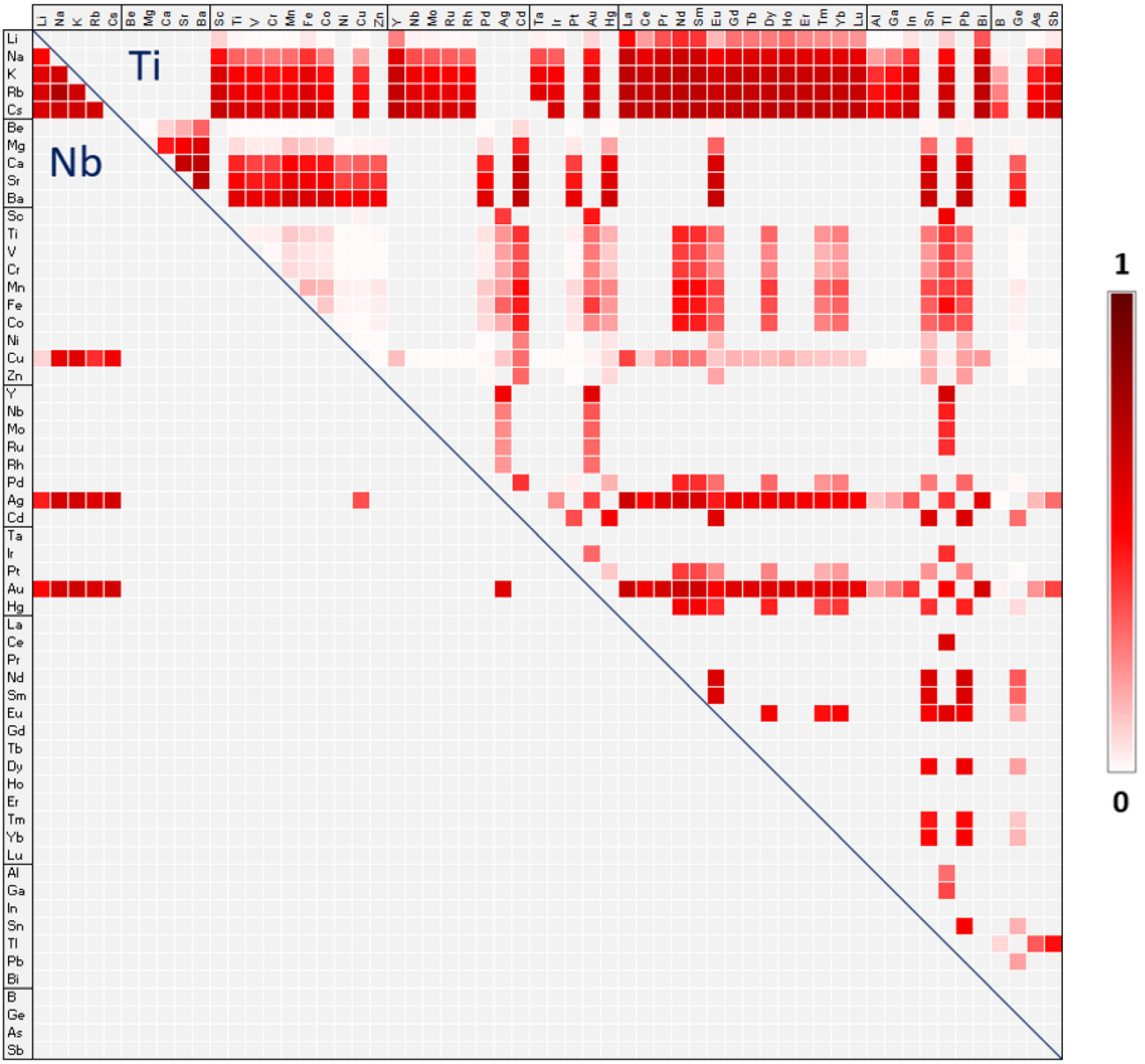


**Fig. 2** Map of the possible A-site double perovskite titanates (upper triangle) and niobates (lower triangle). The color scale gives the probability of forming a perovskite with the formula $AA'(Ti/Nb)_2O_6$. Probabilities have been obtained by fitting the calculated $\tau$ values to the Platt-scaled classification probabilities from Bartel *et al.*[4] The combination of A and A′ ions must provide charge-balanced composition and per definition the average of the ionic radii of A and A′ must be larger than the ionic radius of B.

kites according to ICSD. Most of those, however, show tilting and/or distortion of the $BO_6$ octahedra. So far, nine A-site double perovskites with $\tau > 4.18$ have been synthesized, six of them under high pressure and high temperature. $NaEuTi_2O_6$ has been obtained at atmospheric pressure but high temperature.[41] It is very close to the border of being determined a perovskite with $\tau = 4.182$. The compound $Li_{0.2}Na_{0.8}Nb_2O_3$ [42] is synthesized at atmospheric pressure and 1000 °C, the same as $Li_{0.1}Ag_{0.9}Nb_2O_3$.[43] The small amount of lithium in the compounds explains the rather mild synthesis conditions. Of those combinations with $\tau < 4.18$, we found 30 compounds which were synthesized and characterized but are not perovskites. However, in none of these cases the stoichiometry fits a perovskite-like stoichiometry. It is possible that with the correct stoichiometry and under other synthesis conditions a perovskite would form. Considering the relatively large number of correctly predicted A-site double perovskites, and the fact that perovskites with $\tau > 4.18$ have been synthesized under high pressure, the predictive power of the tolerance factor $\tau$ appears to be rather good also for A-site double perovskites.

Most interesting A-site double perovskites are those where the A and A′ ions order in columnar, planar, or rock-salt ordering.[14] Next, we will investigate how combining the map in Fig. 2 with quantum chemical methods can be used as a start-

 

ing point for exploring new A-site ordered double perovskites. After choosing any potential composition, quantum chemical methods can be used to investigate the structural characteristics and energetics in more detail.

### 3.2. Quantum chemical calculations on potential A-site double perovskites

Looking at Fig. 2 for likely A-site ordered double perovskite compositions, we focus on titanates with alkali metals (+I) on the A-site because they pair with a +III cation on the A′-site, leading to a difference in the oxidation states. This difference enhances the likelyhood of ordering, in particular in combination with matching octahedral tilting, anion vacancies, or second-order Jahn–Teller distortions of B-site cations.[14] Furthermore, we pay attention to the ionic radii. Alkali metals and lanthanides are close in ionic size and King *et al.* found several of them to form stable compounds in their 2007 paper[44] on doubly cation ordered perovskites of the form AA′ $BWO_6$. In fact, King and Garcia-Martin provided in 2019 a list of all known doubly cation ordered perovskites of the form AA′ $BB'O_6$,[21] and almost all compounds in the list have a combination of an alkali metal ion and a lanthanide ion on the A and A′ sites (few compounds with Y(III) cation are included). Perovskites with A-site cations of similar size (*e.g.* Na and La) thus appear to be easier to synthesize. However, in the above-mentioned papers, the focus was on doubly cation ordered perovskites where the different B-site cations can also influence the ordering of the A-site. In their 2010 paper,[14] King and Woodward note the A-site to be more likely to order in a layered fashion if the A-site cations are different in size. Layered ordering is also the most common type of ordering on the A-site. In 2017, Gou *et al.*[45] also suggested that A-site ordering requires a difference in size for the ionic radii.

For the +III cation, we decided to test the predictive power of the $\tau$ tolerance factor for d-metals instead of the more studied lanthanides. Combination of smaller d-metal cation and larger alkali metal cation should promote ordering on the A-site. It can be seen in Fig. 2 that of such combinations, Cs as the A ion and Sc as the A′ ion has one of the highest likelihoods with a $\tau$ value of 3.85. In this composition, there is a large size difference of 1.01 Å in the ionic radii ($r_{Cs}$ = 1.88 Å, $r_{Sc}$ = 0.87 Å). It needs to be mentioned here that these values belong to a twelve coordination of Cs but an eight-coordination of Sc since this is the highest coordination listed by Shannon. BVS-derived 12-coordinated radius for Sc would be 0.96 Å, which would lead to a difference of 0.92 Å and $\tau$ value of 3.82 Å (even higher likelyhood of existence). To put these values in perspective, the largest difference between A and A′ ionic radii in known double perovskite titanates is 0.63 Å in $KCeTi_2O_6$.[46] $CsScTi_2O_6$ has yet not been synthesized according to ICSD.

Another example for a potential A-site ordered double perovskite is $YRbTi_2O_6$, which also has a difference of two in the oxidation states of Y(III) and Rb(I). It has not yet been synthesized according to ICSD. The difference in ionic radius is smaller than in $CsScTi_2O_6$: with $r_Y$ = 1.08 Å and $r_{Rb}$ = 1.72 Å, the difference is only 0.64 Å which is in the range of the ionic size difference in $KCeTi_2O_6$ (0.63 Å, the largest difference between A and A′ ionic radii in known double perovskite titanates). Again, the ionic radius for Rb is given for twelve coordination while the one for Y is in nine coordination. The BVS-derived 12-coordinated ionic radius of Y would be 1.13 Å which leads to a difference of 0.59 Å. For the two radii choices, the $\tau$ values are essentially identical with 3.83 and 3.84, both values suggesting that a perovskite should form.

To sum up, the tolerance factor $\tau$ together with other structural characteristics would suggest $CsSCTi_2O_6$ and $YRbTi_2O_6$ to be A-site ordered double perovskites. We now follow our previous work[38] where we systematically investigated the ordering and Glazer tilt system[47] of A-site ordered double perovskites. We take into account 11 Glazer tilt systems together with columnar, planar, or rock-salt ordering which leaves us with 33 possible crystal structures for each composition. We optimize each crystal structure with DFT-PBE0 method and analyze the resulting structures and energetics.

### 3.3. $CsScTi_2O_6$

In $CsScTi_2O_6$, the A and A′ ion are very different in size, and as a result the $TiO_6$ octahedra are mildly to strongly distorted in most of the 33 crystal structures studied, within the constraints of the space group symmetry. Typically, Glazer tilt systems are built from rigid B-site coordination octahedra (Ti in this case) that can be tilted but not distorted. In some of the optimized crystal structures, the octahedra distort to the point where no octahedra are formed anymore. At the same time in the A-site, the coordination number of Sc can go down to five or even smaller, which is too small for scandium.[27] The lowest-energy crystal structure optimized for $CsScTi_2O_6$ is in space group $Pmc2_1$ in planar A-site ordering, where a $a^-b^+a^-$ tilt system was expected. Fig. 3 shows the calculated structure. It is obvious that the perovskite structure is not the preferred

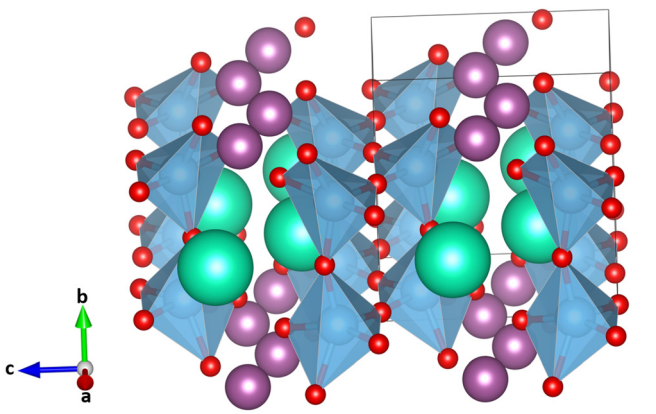


**Fig. 3** Lowest-energy structure of the 33 optimized $CsScTi_2O_6$ crystal structures. Cs(I) cations colored in green, Sc(III) cations in purple, Ti(IV) cations in blue, and O(−II) anions in red. The starting point of the structural optimization was the $a^-b^+a^-$ tilt system in planar A-site ordering with the space group $Pmc2_1$. Lattice parameters *a*, *b*, and *c* have not been constrained during the optimization even though the tilt system would $a^-b^+a^-$ require two lattice parameters to be the same.

structure for this compound since the lowest energy system does not even show the typical octahedra. In fact, the six lowest-energy structures, planar $a^-b^+a^-$, $a^-b^-b^-$, $a^-a^-a^-$ and $a^+b^0c^-$ and rock salt $a^-b^+a^-$ and $a^+b^0c^-$ do not show octahedral coordination of titanium ions. According to Shannon,[27] scandium prefers a coordination of at least six which also is unavailable in many of those low-energy structures. The lowest-energy perovskite-like structure with octahedrally coordinated titanium is planar $a^0b^-b^-$ which can be seen in Fig. 4. It is 114 kJ mol$^{-1}$ higher in energy than the lowest energy structure (Fig. 3) which is a significant difference. A large ionic size difference of the A-site cations might thus undermine the predictive value of the tolerance factor $\tau$ in its current form. Eqn (3) only uses the average ionic radius. There is a possibility that ions which are too different in size will not form a perovskite despite $\tau$ predicting it to be likely.

All in all, the compound $CsScTi_2O_6$ shows the limits of the new tolerance factor $\tau$ for A-site ordered double perovskites for A-site cations with large size difference. It remains to be tested whether $CsScTi_2O_6$ can form a perovskite or not. According to the map in Fig. 2 the compound should form a double perovskite while quantum chemical calculations do not support this prediction.

### 3.4. $YRbTi_2O_6$

Since the large size difference of the A and A′ cations in $CsScTi_2O_6$ caused strong distortion of the octahedra and too small coordination number of the Sc ions in some of the structures, we now look at $YRbTi_2O_6$ ($r_Y$ = 1.08 Å, nine-coordinated radius and $r_{Rb}$ = 1.72 Å, 12-coordinated radius with a difference of 0.64 Å). The results of the calculations can be found in Table 1. The lowest-energy ordering-tilt combination, columnar $a^+b^0c^-$ (space group *Pmm*2), has a long Ti–O distance of 2.99 Å (Fig. 5). Harmonic frequency calculations show the optimized structure to be a true global minimum. The second-lowest energy structure, planar $a^-b^+a^-$, is 35 kJ mol$^{-1}$ higher in energy and exhibits slightly distorted but still perovskite-like $TiO_6$ octahedra (Fig. 6). Table 1 shows that the planar ordering seems to be the lowest-energy ordering for the A-site cations, which is plausible since planar ordering is the most likely for A-site ordered double perovskites.[14] Further research is necessary to determine whether $YRbTi_2O_6$ can form a perovskite structure or not.

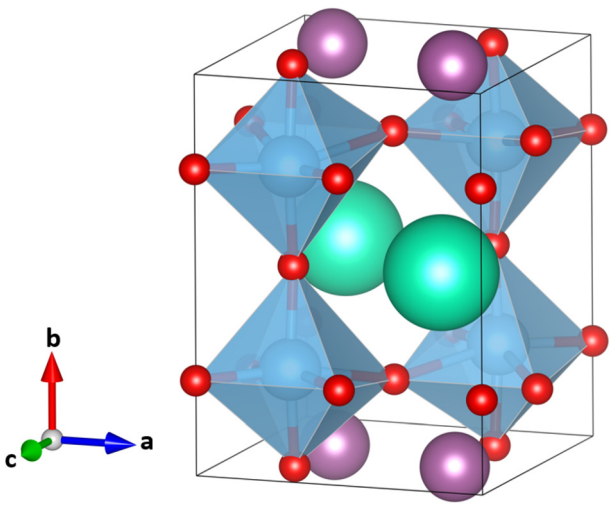


**Fig. 4** Lowest-energy perovskite-like structure of the 33 optimized $CsScTi_2O_6$ crystal structures, retaining the $TiO_6$ octahedra. Cs(I) cations colored in green, Sc(III) cations in purple, Ti(IV) cations in blue, and O(−II) anions in red. In planar A-site ordering and with the tilt system $a^0b^-b^-$ it has the space group *Pmma*. Lattice parameters were not constrained in any way, although in principle the tilt system $a^0b^-b^-$ would require two lattice parameters to be the same.

**Table 1** Summary of the DFT-PBE0 relative energies $E_{rel}$ for different tilt systems and A-site orderings of $YRbTi_2O_6$. Relative energies are given as the difference to the lowest-energy structure. Energies and relative energies are given per formula unit ($Z$). Glazer space group is the space group of the tilt system and double perovskite space group is the space group arising after A-site ordering is applied for the tilt system

| Tilt system | Glazer space group | Double perovskite space group | $E/Z$ [Hartree] | $E_{rel}$ [kJ mol$^{-1}$] |
|---|---|---|---|---|
| **Columnar A-site ordering** | | | | |
| $a^+a^+a^+$ | 204 *Im*$\bar{3}$ | 71 *Immm* | −2212.815026 | 74 |
| $a^+a^+c^-$ | 137 $P4_2/nmc$ | 137 $P4_2/nmc$ | −2212.814905 | 74 |
| $a^-b^+a^-$ | 62 *Pnma* | 11 $P2_1/m$ | −2212.810291 | 86 |
| $a^-b^-b^-$ | 15 *C*2/*c* | 13 *P*2/*c* | −2212.807763 | 93 |
| $a^-a^-a^-$ | 167 *R*$\bar{3}$*c* | 13 *P*2/*c* | −2212.805262 | 100 |
| $a^0b^+b^+$ | 139 *I*4/*mmm* | 139 *I*4/*mmm* | −2212.814899 | 74 |
| $a^+b^0c^-$ | 63 *Cmcm* | 25 *Pmm*2 | −2212.843203 | 0 |
| $a^0b^-b^-$ | 74 *Imma* | 51 *Pmma* | −2212.807772 | 93 |
| $a^0a^0c^+$ | 127 *P*4/*mbm* | 65 *Cmmm* | −2212.802939 | 106 |
| $a^0a^0c^-$ | 140 *I*4/*mcm* | 132 $P4_2/mcm$ | −2212.803378 | 105 |
| $a^0a^0a^0$ | 221 *Pm*$\bar{3}$*m* | 123 *P*4/*mmm* | −2212.797404 | 120 |
| **Planar A-site ordering** | | | | |
| $a^+a^+a^+$ | 204 *Im*$\bar{3}$ | 47 *Pmmm* | −2212.823192 | 53 |
| $a^+a^+c^-$ | 137 $P4_2/nmc$ | 115 *P*$\bar{4}$*m*2 | −2212.823046 | 53 |
| $a^-b^+a^-$ | 62 *Pnma* | 26 $Pmc2_1$ | −2212.830042 | 35 |
| $a^-b^-b^-$ | 15 *C*2/*c* | 13 *P*2/*c*/3 *P*2 | −2212.823397 | 52 |
| $a^-a^-a^-$ | 167 *R*$\bar{3}$*c* | 13 *P*2/*c* | −2212.822985 | 53 |
| $a^0b^+b^+$ | 139 *I*4/*mmm* | 123 *P*4/*mmm* | −2212.821915 | 56 |
| $a^+b^0c^-$ | 63 *Cmcm* | 38 *Amm*2 | −2212.826897 | 43 |
| $a^0b^-b^-$ | 74 *Imma* | 51 *Pmma* | −2212.823317 | 52 |
| $a^0a^0c^+$ | 127 *P*4/*mbm* | 65 *Cmmm* | −2212.815461 | 73 |
| $a^0a^0c^-$ | 140 *I*4/*mcm* | 125 *P*4/*nbm* | −2212.821135 | 58 |
| $a^0a^0a^0$ | 221 *Pm*$\bar{3}$*m* | 123 *P*4/*mmm* | −2212.820837 | 59 |
| **Rock salt A-site ordering** | | | | |
| $a^+a^+a^+$ | 204 *Im*$\bar{3}$ | 200 *Pm*$\bar{3}$ | −2212.783521 | 157 |
| $a^+a^+c^-$ | 137 $P4_2/nmc$ | 115 *P*$\bar{4}$*m*2 | −2212.795828 | 124 |
| $a^-b^+a^-$ | 62 *Pnma* | 31 $Pmn2_1$ | −2212.802313 | 107 |
| $a^-b^-b^-$ | 15 *C*2/*c* | 5 *C*2 | −2212.798448 | 118 |
| $a^-a^-a^-$ | 167 *R*$\bar{3}$*c* | 5 *C*2 | −2212.801118 | 110 |
| $a^0b^+b^+$ | 139 *I*4/*mmm* | 123 *P*4/*mmm* | −2212.786199 | 150 |
| $a^+b^0c^-$ | 63 *Cmcm* | 38 *Amm*2 | −2212.803817 | 103 |
| $a^0b^-b^-$ | 74 *Imma* | 44 *Imm*2 | −2212.798429 | 118 |
| $a^0a^0c^+$ | 127 *P*4/*mbm* | 136 $P4_2/mnm$ | −2212.785915 | 150 |
| $a^0a^0c^-$ | 140 *I*4/*mcm* | 121 $I\bar{4}_2m$ | −2212.795261 | 126 |
| $a^0a^0a^0$ | 221 *Pm*$\bar{3}$*m* | 225 *Fm*$\bar{3}$*m* | −2212.766282 | 202 |

### 3.5. $YKTi_2O_6$

It seems that despite the clear indication of the low $\tau$ value (Fig. 2), neither $CsScTi_2O_6$ nor $YRbTi_2O_6$ can be expected to be a double perovskite with high confidence. To study whether

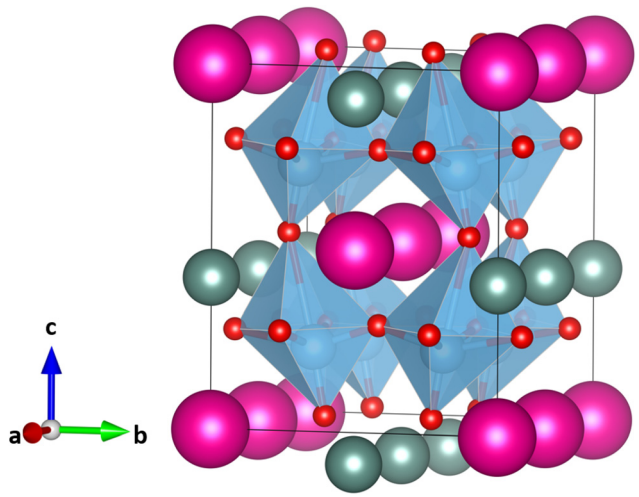


Fig. 5 Lowest-energy perovskite-like structure of the 33 calculated $YRbTi_2O_6$ structures with Y(III) cations colored in grey, Rb(I) cations in pink, Ti(IV) cations in blue, and O(−II) anions in red. In columnar A-site ordering and with the tilt system $a^+b^0c^-$ the space group is *Pmm*2.

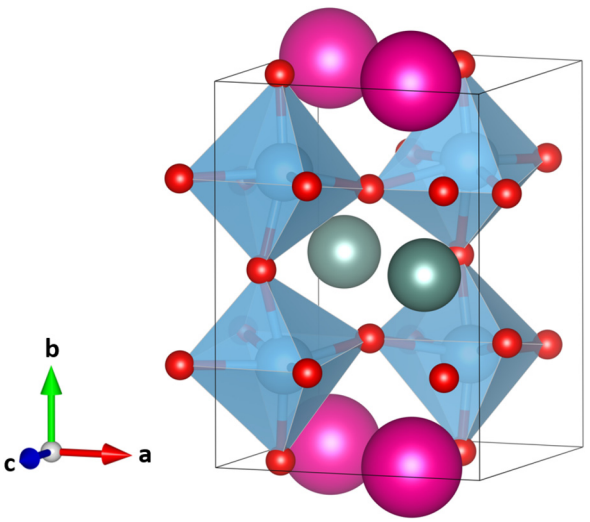


Fig. 6 Second-lowest energy perovskite-like structure of the 33 calculated $YRbTi_2O_6$ structures with Y(III) cations colored in grey, Rb(I) cations in pink, Ti(IV) cations in blue, and O(−II) anions in red. In planar A-site ordering and with the tilt system $a^-b^+a^-$ the space group is $Pmc2_1$. The structure is 35 kJ mol$^{-1}$ higher in energy compared to the lowest-energy structure in Fig. 5.

the difference in size between the two A-site ions causes the strongly distorted structures, we next studied $YKTi_2O_6$. Potassium cations have similar chemical properties to rubidium cations, but are smaller in size ($r_K$ = 1.64 Å, 12-coordinated radius) and therefore closer to yttrium ($r_Y$ = 1.08 Å, nine-coordinated radius). The combination of Y and K even has already been found in the doubly cation ordered perovkite $KYCaWO_6$.[21] There have, however, not yet been found any compounds with Y and Rb or Y and Cs on the A-site. For comparison, Fig. 7 shows $YKTi_2O_6$ in space group *Pmm*2, the same

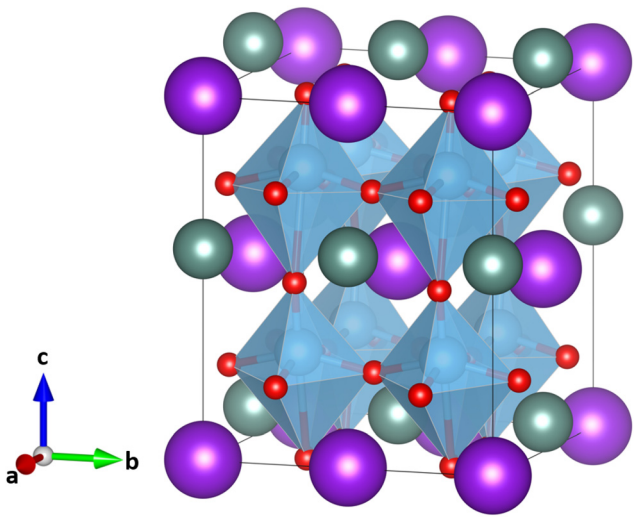


Fig. 7 $YKTi_2O_6$ structure with Y(III) cations in grey, K(I) cations in dark purple, Ti(IV) cations in blue, and O(−II) anions red. In columnar A-site ordering and with the tilt system $a^+b^0c^-$ it has the space group *Pmm*2, the same space group as the lowest-energy structure of $YRbTi_2O_6$.

space group as the lowest-energy system of $YRbTi_2O_6$ (Fig. 5). Again, frequency calculations show the structure to be true local minimum. The oxygen octahedra are still distorted but the maximum Ti–O distance decreases to 2.78 Å. This composition might not be any more likely to exist as a double perovskite, but it is another indicator that ionic sizes play a large role in A-site double perovskites. According to $\tau$, $YRbTi_2O_6$ ($\tau$ = 3.83), is more likely to form a double perovskite than $YKTi_2O_6$ ($\tau$ = 3.87), but according to quantum chemical calculations, $YKTi_2O_6$ would seem somewhat more likely to form a double perovskite. Another point to consider is that the probability of A-site ordering decreases with the smaller size difference of the A-site cations.

The reason why the new tolerance factor $\tau$ works fairly well on B-site ordered double perovskites[4] but needs the support of quantum chemical calculations for A-site double perovskites can be found in the class of elements which are typically found on these sites. The B-site typically is occupied by d-metal ions, which do not vary much in size from one element to another and are overall on the smaller side. On the A-site, however, large number of elements around the periodic table can be found. Especially the large alkali metal ions paired with small d-metal ions come out as medium ionic sizes when the radii are averaged which for the calculation of $\tau$. These medium ionic sizes then lead to high probabilities of double perovskite, even though the combination of A-site ions is not actually likely to lead in a double perovskite structure.

## 4. Conclusions

The new tolerance factor $\tau$ can be used to screen all possible and feasible combination for A-site double perovskite oxides. Here the screening was carried out for double perovskite tita-

nates and niobates The predictive power of $\tau$ is relatively good based on comparisons with available experimental data for A-site double perovskites. However, we found limitations for the use of the new tolerance factor for A-site double perovskites where the A and A′ ions are very different in size. Quantum chemical calculations on $CsScTi_2O_6$ have shown that the huge size difference of Cs and Sc leads to strongly distorted oxygen octahedra and the resulting lowest-energy structures are no longer perovskite-like. According to $\tau$, $YRbTi_2O_6$ also had a rather high probability to form a perovskite, but with a smaller difference in ionic radii of A-site cations compared to $CsScTi_2O_6$. Consequently, quantum chemical calculations suggest a somewhat distorted, but still perovskite-like structure as the lowest-energy structure. The distortion further decreases when moving to $YKTi_2O_6$. This finding is in line with experimental observation of doubly cation ordered perovskite $KYCaWO_6$.

Overall, the new tolerance factor $\tau$ provides a reasonable starting point for the search of new A-site (ordered) double perovskites. However, consideration of tilt systems with the help of quantum chemical calculations is still necessary to make more robust predictions. In the future, the predictive power of $\tau$ can be investigated more extensively when more experimental data on novel A-site double perovskites becomes available.

## Author contributions

Elisabeth K. Albrecht: Conceptualization; investigation; visualization; writing – original draft preparation; writing – review and editing. Antti. J. Karttunen: Conceptualization; writing – review and editing; supervision; funding acquisition. All authors have read and agreed to the published version of the manuscript.

## Conflicts of interest

There are no conflicts to declare.

## Acknowledgements

We thank Dawid Stryszyk for his data mining work, the Academy of Finland for funding (grant no. 317273), and CSC – The Finnish IT Center for Science for computational resources.

## References

1 R. J. D. Tilley, *Perovskites: structure-property relationships*, Wiley, Chichester, West Sussex, United Kingdom, 1st edn, 2016.
2 V. M. Goldschmidt, *Naturwissenschaften*, 1926, **14**, 477–485.
3 C. Li, K. C. K. Soh and P. Wu, *J. Alloys Compd.*, 2004, **372**, 40–48.
4 C. J. Bartel, C. Sutton, B. R. Goldsmith, R. Ouyang, C. B. Musgrave, L. M. Ghiringhelli and M. Scheffler, *Sci. Adv.*, 2019, **5**, eaav0693.
5 R. Ouyang, S. Curtarolo, E. Ahmetcik, M. Scheffler and L. M. Ghiringhelli, *Phys. Rev. Mater.*, 2018, **2**, 083802.
6 J. C. Platt, *Advances in Large-Margin Classifiers*, The MIT Press, 1999, vol. 10, pp. 61–74.
7 M. R. Filip and F. Giustino, *Proc. Natl. Acad. Sci. U. S. A.*, 2018, **115**, 5397–5402.
8 K. Momma and F. Izumi, *J. Appl. Crystallogr.*, 2011, **44**, 1272–1276.
9 L. Schneemeyer, J. Waszczak, S. Zahorak, R. van Dover and T. Siegrist, *Mater. Res. Bull.*, 1987, **22**, 1467–1473.
10 B. Raveau, A. Maignan, C. Martin and M. Hervieu, *Chem. Mater.*, 1998, **10**, 2641–2652.
11 G. Hodes, *Science*, 2013, **342**, 317–318.
12 S. Vasala and M. Karppinen, *Prog. Solid State Chem.*, 2015, **43**, 1–36.
13 M. C. Knapp and P. M. Woodward, *J. Solid State Chem.*, 2006, **179**, 1076–1085.
14 G. King and P. M. Woodward, *J. Mater. Chem.*, 2010, **20**, 5785.
15 M. W. Lufaso, P. W. Barnes and P. M. Woodward, *Acta Crystallogr., Sect. B: Struct. Sci.*, 2006, **62**, 397–410.
16 C. Bernuy-Lopez, K. Høydalsvik, M.-A. Einarsrud and T. Grande, *Materials*, 2016, **9**, 154.
17 F. J. Garcia-Garcia, M. J. Sayagués and F. J. Gotor, *Nanomaterials*, 2021, **11**, 380.
18 R. Ghosh, A. Barik, M. R. Sahoo, S. Tiwary, P. D. Babu, S. D. Kaushik and P. N. Vishwakarma, *J. Appl. Phys.*, 2022, **132**, 224107.
19 M. Goto, T. Saito and Y. Shimakawa, *Chem. Mater.*, 2018, **30**, 8702–8706.
20 B. Jiang, T. M. Raeder, D.-Y. Lin, T. Grande and S. M. Selbach, *Chem. Mater.*, 2018, **30**, 2631–2640.
21 G. King and S. Garcia-Martin, *Inorg. Chem.*, 2019, **58**, 14058–14067.
22 G. King, S. Garcia-Martin, E. Urones-Garrote, G. Nenert and P. M. Woodward, *Additional Conferences (Device Packaging, HiTEC, HiTEN, and CICMT)*, 2013, **2013**, 000006–000013.
23 S. S. Pramana, A. Cavallaro, C. Li, A. D. Handoko, K. W. Chan, R. J. Walker, A. Regoutz, J. S. Herrin, B. S. Yeo, D. J. Payne, J. A. Kilner, M. P. Ryan and S. J. Skinner, *J. Mater. Chem. A*, 2018, **6**, 5335–5345.
24 K. Świerczek, A. Klimkowicz, K. Zheng and B. Dabrowski, *J. Solid State Chem.*, 2013, **203**, 68–73.
25 J. Young and J. M. Rondinelli, *Phys. Rev. B: Condens. Matter Mater. Phys.*, 2014, **89**, 174110.
26 Y. Zhang, H. Zhao, Z. Du, K. Świerczek and Y. Li, *Chem. Mater.*, 2019, **31**, 3784–3793.
27 R. D. Shannon, *Acta Crystallogr., Sect. A: Cryst. Phys., Diffr., Theor. Gen. Crystallogr.*, 1976, **32**, 751–767.
28 I. D. Brown, *Chem. Rev.*, 2009, **109**, 6858–6919.
29 D. Brown and M. W. Lufaso, Bond valence parameters (bvparm2020.cif, accessed 2023-08-07), **https://www.iucr.org/resources/data/datasets/bond-valence-parameters**.

30 D. Zagorac, H. Müller, S. Ruehl, J. Zagorac and S. Rehme, *J. Appl. Crystallogr.*, 2019, **52**, 918–925.
31 R. Dovesi, A. Erba, R. Orlando, C. M. Zicovich-Wilson, B. Civalleri, L. Maschio, M. Rérat, S. Casassa, J. Baima, S. Salustro and B. Kirtman, *Wiley Interdiscip. Rev.: Comput. Mol. Sci.*, 2018, **8**, 1–36.
32 J. P. Perdew, K. Burke and M. Ernzerhof, *Phys. Rev. Lett.*, 1996, **77**, 3865–3868.
33 C. Adamo and V. Barone, *J. Chem. Phys.*, 1999, **110**, 6158–6170.
34 F. Weigend and R. Ahlrichs, *Phys. Chem. Chem. Phys.*, 2005, **7**, 3297–3305.
35 M. S. Kuklin, K. Eklund, J. Linnera, A. Ropponen, N. Tolvanen and A. J. Karttunen, *Molecules*, 2022, **27**, 874.
36 R. E. Stene, B. Scheibe, A. J. Karttunen, W. Petry and F. Kraus, *Eur. J. Inorg. Chem.*, 2019, **2019**, 3672–3682.
37 H. J. Monkhorst and J. D. Pack, *Phys. Rev. B: Solid State*, 1976, **13**, 5188–5192.
38 E. K. Albrecht and A. J. Karttunen, *Dalton Trans.*, 2022, **51**, 16508–16516.
39 F. Pascale, C. M. Zicovich-Wilson, F. López Gejo, B. Civalleri, R. Orlando and R. Dovesi, *J. Comput. Chem.*, 2004, **25**, 888–897.
40 C. M. Zicovich-Wilson, F. Pascale, C. Roetti, V. R. Saunders, R. Orlando and R. Dovesi, *J. Comput. Chem.*, 2004, **25**, 1873–1881.
41 R. Ranjan, A. Senyshyn, H. Boysen, C. Baehtz and F. Frey, *J. Solid State Chem.*, 2007, **180**, 995–1001.
42 C. A. L. Dixon, J. A. McNulty, S. Huband, P. A. Thomas and P. Lightfoot, *IUCrJ*, 2017, **4**, 215–222.
43 U. Farid, H. U. Khan, M. Avdeev, T. A. Whittle and B. J. Kennedy, *J. Solid State Chem.*, 2019, **269**, 401–408.
44 G. King, S. Thimmaiah, A. Dwivedi and P. M. Woodward, *Chem. Mater.*, 2007, **19**, 6451–6458.
45 G. Gou, N. Charles, J. Shi and J. M. Rondinelli, *Inorg. Chem.*, 2017, **56**, 11854–11861.
46 J. Brous, I. Fankuchen and E. Banks, *Acta Crystallogr.*, 1953, **6**, 67–70.
47 A. M. Glazer, *Acta Crystallogr., Sect. B: Struct. Crystallogr. Cryst. Chem.*, 1972, **28**, 3384–3392.